DMD Fast Forward. Published on January 20, 2021 as DOI: 10.1124/dmd.120.000057
This article has not been copyedited and formatted. The final version may differ from this version.

Function and Expression of Bile Salt Export Pump in Suspension Human Hepatocytes

Paresh P. Chothe[*1,2], Rachel Pemberton[1] and Niresh Hariparsad[1,3]

[1]Drug Metabolism and Pharmacokinetics, Vertex Pharmaceuticals Incorporated, Boston, Massachusetts, USA

[2]Current affiliation - Drug Metabolism and Pharmacokinetics, Takeda Pharmaceutical Company Limited, Cambridge, Massachusetts, USA

[3]Current affiliation - Drug Metabolism and Pharmacokinetics, AstraZeneca, 35 Gate House Park, Waltham, Massachusetts, USA

DMD Fast Forward. Published on January 20, 2021 as DOI: 10.1124/dmd.120.000057
This article has not been copyedited and formatted. The final version may differ from this version.

Running title: BSEP Function in Suspension Hepatocytes

***Corresponding Authors:**

Paresh P. Chothe, Ph.D.

Department of Drug Metabolism and Pharmacokinetics

35 Landsdowne Street, Cambridge, MA 02139

Phone: +1-706-504-5888

E-mail: paresh.chothe@takeda.com

Pages: 37

Tables: 2

Figures: 4

References: 43

Number of words in Abstract: 246

Number of words in Introduction: 681

Number of in Discussion: 1802

Abbreviations

BSEP, bile salt extrusion pump; CA, cholic acid; CDCA, chenodeoxycholic acid; CsA, cyclosporine A; DHEAS, dehydroepiandrosterone sulfate; G-CA, glycocholic acid; G-CDCA, glycochenodeoxycholic acid; MRP, multidrug resistance-associated protein; NTCP, Na^+/ taurocholate co-transporting polypeptide; OATP, organic anion transporting polypeptide; OSTα/β, organic solute transporter alpha/beta; SHH, suspension human hepatocytes; SCHH, sandwich-cultured human hepatocytes; T-CA, taurocholic acid; T-CDCA, taurochenodeoxycholic acid.

DMD Fast Forward. Published on January 20, 2021 as DOI: 10.1124/dmd.120.000057
This article has not been copyedited and formatted. The final version may differ from this version.

Abstract

The mechanistic understanding of bile salt disposition is not well established in suspension human hepatocytes (SHH) due to limited information on the expression and function of bile salt export protein (BSEP) in this system. We investigated the transport function of BSEP in SHH using a method involving *in situ* biosynthesis of bile salts from their precursor bile acids, cholic acid (CA) and chenodeoxycholic acid (CDCA). Our data indicated that glycine and taurine-conjugated CA and CDCA were generated efficiently and transported out of hepatocytes in a concentration-and time-dependent manner. We also observed that the membrane protein abundance of BSEP was similar between SHH and sandwich cultured human hepatocytes. Furthermore, known cholestatic agents significantly inhibited G-CA and G-CDCA efflux in SHH. Interestingly, cyclosporine A, troglitazone, itraconazole, loratadine and lovastatin inhibited G-CA efflux more potently than G-CDCA efflux (3-5-fold). Due to these significant differential effects on G-CA and G-CDCA efflux inhibition, we determined the IC_{50} values of troglitazone for G-CA (9.9 µM) and for G-CDCA (43.1 µM) efflux. The observed discrepancy in the IC_{50} was attributed to the fact that troglitazone also inhibits organic anion transporting polypeptide (OATP)s and Na^+/ taurocholate co-transporting polypeptide (NTCP) in addition to BSEP. The hepatocyte uptake study suggested that both active uptake and passive diffusion contribute to the liver uptake of CA while CDCA primarily undergoes passive diffusion into the liver. In summary, these data demonstrated the expression and function of BSEP and its major role in transport of bile salts in cryopreserved SHH.

DMD Fast Forward. Published on January 20, 2021 as DOI: 10.1124/dmd.120.000057
This article has not been copyedited and formatted. The final version may differ from this version.

Statement of Significance

BSEP transport function and protein abundance was evident in SHH in the present study. The membrane abundance of BSEP protein was similar between SHH and SCHH. The study also illustrated the major role of BSEP relative to basolateral MRP3 and MRP4 in transport of bile salts in SHH. Understanding of BSEP function in SHH may bolster the utility of this platform in mechanistic understanding of bile salt disposition and potentially in the assessment of drugs for BSEP inhibition.

DMD Fast Forward. Published on January 20, 2021 as DOI: 10.1124/dmd.120.000057
This article has not been copyedited and formatted. The final version may differ from this version.

Introduction

Primary human hepatocytes (either freshly isolated or cryopreserved) in suspension is considered the gold standard for the assessment of metabolic and uptake clearance(Soars et al., 2007; Zhao, 2008; Chiba et al., 2009; Yang et al., 2016) as they maintain both uptake transporter and metabolic enzyme activity(Gomez-Lechon et al., 2004; Richert et al., 2006; Keemink et al., 2018). However, their utilization for the assessment of bile salt disposition which is critical in the mechanistic understanding of cholestasis and drug-induced liver injury (DILI) has remained questionable due to the belief that canalicular transporters lose their membrane expression (internalized) during the process of hepatocyte isolation. This is evident from the study by Bow D et. al. who showed that P-gp and Mrp2 proteins are internalized and not localized in the canalicular membrane of freshly isolated rat hepatocytes and therefore suspension hepatocytes do not represent a good model to study canalicular excretion of drugs (Bow et al., 2008). On the contrary, Li M et. al. and Lundquist P. et. al. showed that bile canalicular efflux transporters including P-gp, BCRP, BSEP and MRP2 are expressed in the plasma membrane of freshly isolated and cryopreserved human hepatocytes (Li et al., 2008; Lundquist et al., 2014). Furthermore, Li M. et. al. showed the efflux activity of P-gp, BCRP and MRP2 in SHH using 3,3′-diethyloxacarbocyanine iodide (DiOC2(3)), Pheophorbide A (PhA) and glutathione methylfluorescein (GS-MF) (derived from 5-Chloromethylfluoresceindiacetate (CMFDA), respectively while Lundquist P et. al. demonstrated P-gp and BCRP efflux activity in SHH by inhibiting efflux of fexofenadine and rosuvastatin in the presence of elacridar (P-gp inhibitor) and fumitremorgin C (FTC) (BCRP inhibitor), respectively. Thus, in contrast to Bow D et. al. data from Lundquist P et. al. indicated that only a fraction of canalicular transporters is internalized leaving a

DMD Fast Forward. Published on January 20, 2021 as DOI: 10.1124/dmd.120.000057
This article has not been copyedited and formatted. The final version may differ from this version.

significant portion of transporter proteins in the canalicular plasma membrane of freshly isolated and cryopreserved human hepatocytes (Lundquist et al., 2014).

Recently Zhang J et. al. and Yucha R et. al. showed the efflux of G-CA and G-CDCA in SHH and suggested that BSEP is the primary pathway responsible for the efflux of these bile salts out of human hepatocytes (Zhang et al., 2016; Yucha et al., 2017). However, this study did not account for the involvement of basolateral efflux transporters such as MRP3, MRP4 and OSTα/β which are known to be involved in the transport of bile salts (Zelcer et al., 2003; Rius et al., 2006; Suga et al., 2019). In addition, the study did not provide quantitative information on the membrane protein abundance of BSEP in SHH. In 2009 Li M et. al. quantitively measured the absolute protein abundance of canalicular efflux transporters including BCRP, BSEP and MRP2 in freshly and cryopreserved human hepatocytes in comparison to liver tissues by LC-MS/MS. Interestingly, the protein expression of BCRP, BSEP and MRP2 in both freshly and cryopreserved human hepatocytes was found to be similar to liver tissues (Li et al., 2009a; Li et al., 2009b). Very recently Kumar V et. al. reported total as well as plasma membrane abundance of canalicular transporters including P-gp, MRP2 and BSEP in suspended, plated and sandwich cultured human hepatocytes in direct comparison with human liver tissue by quantitative targeted proteomics (Kumar et al., 2019). In this study, the total membrane abundance of BSEP in SHH and SCHH was found to be similar to liver tissue. Furthermore, the plasma membrane abundance of BSEP was similar between SHH and SCHH although most of it was intracellular. Collectively all previous studies looked at either the plasma membrane expression or the transport activity of BSEP separately but did not comprehensively investigate BSEP expression,

DMD Fast Forward. Published on January 20, 2021 as DOI: 10.1124/dmd.120.000057
This article has not been copyedited and formatted. The final version may differ from this version.

function and its relative contribution to bile salt transport in comparison to basolateral MRP3, MRP4 and OSTα/β in SHH. Therefore, the objectives of this present study were 3-fold; 1) examine the role of BSEP in the efflux of bile salts in SHH, 2) investigate the involvement of basolateral efflux transporters, MRP3 and MRP4, in the efflux of bile salts in SHH and, 3) quantitatively measure the membrane protein abundance of BSEP in SHH in direct comparison to SCHH using the same lot of human hepatocytes.

DMD Fast Forward. Published on January 20, 2021 as DOI: 10.1124/dmd.120.000057
This article has not been copyedited and formatted. The final version may differ from this version.

Materials and Methods

Transporter-qualified cryopreserved human hepatocyte single donor lot (WWQ) and cryopreserved 5-donor pooled human hepatocyte lot (YZG) were obtained from BIOIVT (Baltimore, MD USA) (Supplemental Table 1). Williams' E medium, recovery medium, hepatocyte maintenance medium and plating medium were purchased from Thermo Fisher (Waltham, MA USA). Atorvastatin, estradiol-17 β-glucuronide, taurocholate, rifamycin SV (RFV), cyclosporin A, itraconazole, reserpine, bosentan, troglitazone, simvastatin, loratadine, valinomycin, lovastatin and MK571 were purchased from Sigma-Aldrich (St. Louis, MO USA). Cholic acid (CA) and chenodeoxycholic acid (CDCA) were procured from IsoScience LLC (Ambler, PA USA). Hepatitis B virus (HBV) peptide was custom synthesized by New England Peptide (Gardner, MA USA). The amino acid sequence of the peptide was derived from the preS1 region of HBV (D-type, GenBank accession number U9555.1) containing residues 2-48 which was modified with N-terminal myristoylation (Konig et al., 2014; Yan et al., 2014). All organic solvents of high quality grade were procured from either Thermo Fisher (Waltham, MA USA) or Sigma-Aldrich (St. Louis, MO USA).

Uptake Assay in Suspension Human Hepatocytes

The conventional oil-spin method was used for the uptake analysis as previously described (Chothe et al., 2018). First, cryopreserved hepatocytes were recovered by thawing them at 37°C and suspending them in hepatocyte recovery medium. Subsequently cells were centrifuged at 100g for 10 min and resuspended in Krebs-Henseleit Buffer (KHB) at a density of 1×10^6 cells/ml. The total (active + passive) uptake of bile acids was measured by incubating hepatocytes at 37°C. For inhibition

DMD Fast Forward. Published on January 20, 2021 as DOI: 10.1124/dmd.120.000057
This article has not been copyedited and formatted. The final version may differ from this version.

study, hepatocytes were pre-incubated with an inhibitor (20 µM RFV, 0.1 µM HBV peptide) for 10 min at 37°C. DMSO (final concentration <1%) was used for pre-incubation as a vehicle control. Each bile acid is then added in to hepatocytes suspension at the desired concentration. Samples were withdrawn at 0.5, 1.5 and 3 min and transferred to centrifuge tubes containing mineral oil and 1 M sucrose. Cells were centrifuged at 10,000 rpm for 15 seconds to terminate the uptake. The centrifuge tubes were kept on dry ice and cut to separate cell pellets which were then collected in cluster tubes. Cell pellets were then lysed by adding 300 µL acetonitrile (containing internal standard). Finally, samples were centrifuged and supernatant was collected to measure the intracellular amount of bile acid by LC-MS/MS.

Efflux Studies in Suspension Human Hepatocytes

Cryopreserved hepatocytes were thawed and recovered as described above. Hepatocytes were reconstituted in hepatocyte maintenance medium at a final density of 0.25×10^6 viable cells/ml as reported previously(Zhang et al., 2016). Cells were incubated at 37°C in the absence and presence of CA or CDCA at 1, 5 and 10 µM concentrations. Aliquots were taken at 15, 30, 60 and 120 minutes and transferred to centrifuge tubes containing mineral oil and 1 M sucrose. Aliquots of supernatants were transferred to a 96-well sample plate for the analysis of effluxed glycine- and taurine-conjugated CA and CDCA by LC-MS/MS.

Transport Studies Using Membrane Vesicles

Human BSEP, MRP3 and MRP4 membrane vesicles studies were conducted at SOLVO Biotechnology at Charles River Company (Hungary). These inside out

DMD Fast Forward. Published on January 20, 2021 as DOI: 10.1124/dmd.120.000057
This article has not been copyedited and formatted. The final version may differ from this version.

membrane vesicles were derived from HEK293 cells expressing BSEP, MRP3 and MRP4. Membrane vesicles were prepared and characterized by SOLVO Biotechnology according to standard operating procedures. The vesicle transport assays were performed in 96-well plates. For both BSEP and MRP vesicle assay, 50 µg of vesicles was mixed with different concentrations of bile salts (G-CA, T-CA, G-CDCA and T-CDCA) and incubated at 37 °C for 10 min. The uptake reaction was initiated by adding MgATP (or MgAMP) at a final concentration of 4mM. Subsequently the assay mixture was incubated at 37 °C for 10 min. The transport reaction was stopped by adding 200 µL ice-cold wash buffer and samples were transferred to pre-wet 96-well glass-fiber filter plates. Filters were washed 3 times with ice cold termination buffer by suctioning. The compound in vesicles is then eluted with 100 µL acetonitrile containing internal standard and subsequently analyzed by LC-MS/MS to quantify BSEP-mediated uptake. The uptake rate was determined using the following equation.

$$Uptake = \frac{amount\ in\ vesicle\ (pmol)}{mg\ protein}$$

The uptake of estradiol-17β-glucuronide, dehydroepiandrosterone sulfate (DHEAS) and TCA was carried out as a positive control substrates in MRP3, MRP4 and BSEP vesicles, respectively. The amount of each positive control substrate inside the filtered vesicles was determined by liquid scintillation counting.

MDCK Permeability Assay

The permeability of CA, CDCA and their glycine- and taurine-conjugated moieties (G-CA, T-CA, G-CDCA and T-CDCA) was assessed in MDCK cells. The procedure was used as described in our earlier report (Moore et al., 2016) using a Tecan Genesis

DMD Fast Forward. Published on January 20, 2021 as DOI: 10.1124/dmd.120.000057
This article has not been copyedited and formatted. The final version may differ from this version.

automated liquid handler (Durham, NC). To perform apical-to-basolateral (A>B) and basolateral-to-apical (B>A) permeability assessment, compounds were added to the donor compartments (1 µM) and HBSS buffer was added to the receiver compartments. The incubations were performed at 37°C for 60 minutes. Samples were withdrawn at 0 and 60 minutes from the receiver and donor compartments and analyzed by LC-MS/MS. At the end of the assay, cells were further incubated with lucifer yellow (100 *µ*M) to assess the integrity of the MDCK cell monolayer.

The apparent permeability coefficient (P_{app}) of bile acids and bile salts was determined using the following equation:

$$Papp = (dQ/dt)/(area \times Co)$$

where *d*Q/*d*t is the rate of transfer of a compound across the cells; area is the surface area of the membrane (0.143 cm^2); and C_0 is the donor concentration of a compound at time zero.

LC-MS/MS Analysis

The quantitative analysis of the analytes was performed using AB Sciex API 5500 mass spectrometer coupled with CTC Analytics PAL autosampler (CTC Analytics AG, Zwingen, Switzerland) in electrospray ionization (ESI) mode.

Analytes were resolved on a Unisol C18 2.1 × 30 mm, 5 µM column (Agela Technologies, Newark, DE) using the mobile phase of 10 mM ammonium acetate in water (pH 4.0, A) and acetonitrile/methanol (50/50, v/v, B) at the flow rate of 0.8 ml/min. The linear gradient was 0.0–0.3 minutes, 0–70% B; 0.3–1.0 minutes, 70%–70% B; 1.0–1.2 minutes, 70%–99% B; 1.2–2.2 minutes, 99%–99% B. The MRM transitions of the

DMD Fast Forward. Published on January 20, 2021 as DOI: 10.1124/dmd.120.000057
This article has not been copyedited and formatted. The final version may differ from this version.

compounds are indicated in Supplemental Table 2. Data analysis was done using Analyst version 1.6.2 (SCIEX, Framingham, MA, USA).

Quantification of Major Liver Uptake and Efflux Transporters in SHH and SCHH

The procedure of the membrane fraction preparation and quantitative analysis of drug transporter protein abundance was followed as described by Khatri R et.al. (Khatri et al., 2019).

Membrane Fractions preparation

Membranes fractions from SHH and SCHH were prepared using Mem-PER^{TM} Plus membrane protein extraction kit (Rockford, IL). Cryopreserved human hepatocytes were recovered as described earlier (Uptake Assay in Human Hepatocytes). About 8 million viable human hepatocytes were used to prepare membrane fractions. For SCHH, cells were scraped from 24-well plate (5th day culture) and collected in 15 ml tubes. Both cryopreserved human hepatocytes and SCHH samples were then processed using the manufacturer's protocol to obtain membrane fractions.

Quantification of Protein Abundance of Drug Transporters

20 µg of total membrane protein was used in the digestion reaction. The samples were solubilized in 1% sodium deoxycholate which helps in the solubilization and denaturation of protein. Membrane protein was transferred to the PCR tubes and evaporated to dryness in a ThermoSavant SpeedVac. The dried protein samples were then denatured and reduced in the presence of 50 mM ammonium bicarbonate, 40 mM dithiothreitol, β-casein and 10 % sodium deoxycholate for 40 min at 60 ^{o}C in an Isotemp Thermal Mixer (Fisher Scientific, Pittsburg, PA). Subsequently, the samples were

DMD Fast Forward. Published on January 20, 2021 as DOI: 10.1124/dmd.120.000057
This article has not been copyedited and formatted. The final version may differ from this version.

incubated with 135 mM iodoacetamide for 30 min in the dark. Each heavy labeled peptide (1 pmol) was then added in tubes. Samples were then digested in the presence of trypsin. The reaction was terminated by adding 10% trifluoroacetic acid and the samples were centrifuged at 13.3K x *g* for 5 min. The supernatant was then treated with solid phase extraction. Elution was done using acetonitrile:formic acid (60:40). Subsequently, the eluate was evaporated to dryness and reconstituted in modified mobile phase A (0.1 % formic acid/acetonitrile, 98:2). The samples were centrifuged at 13.3K x *g* for 5 min and the supernatant was transferred to deactivated vial inserts for LC-MS/MS analysis. Analysis was done using nanoACQUITY (Waters, Milford, MA) coupled with a SCIEX QTRAP 5500 hybrid mass spectrometer (Framingham, MA) equipped with a NanoSpray III source as described by Khatri R. et. al.(Khatri et al., 2019). The peptide sequence and the MRMs for each heavy labeled peptide are shown in Supplemental Table 3.

Data Analysis

The uptake data in human hepatocytes and MRP3, MRP4 and BSEP vesicles was analyzed with One-way ANOVA with Dunnett's comparisons test. The data was considered statistically significant when $p \leq 0.05$. The half-maximal inhibitory concentration (IC_{50}) was troglitazone was determined by fitting data using nonlinear regression equation in GraphPad Prism 8 software.

Results

Measurement of the Efflux of Glycine- and Taurine-conjugated CA and CDCA in SHH

DMD Fast Forward. Published on January 20, 2021 as DOI: 10.1124/dmd.120.000057
This article has not been copyedited and formatted. The final version may differ from this version.

The efflux of G-CA, T-CA, G-CDCA and T-CDCA was measured in two different lots of hepatocytes; cryopreserved 5-donor pooled human hepatocyte lot (YZG) and transporter-qualified cryopreserved human hepatocyte single donor lot (WWQ). CA and CDCA were incubated with SHH at 1, 5 and 10 µM concentrations. The efflux of G-CA, T-CA and G-CDCA and T-CDCA was measured as described in 'materials and method'. The efflux of both glycine- and taurine-conjugated CA and CDCA (G-CA, T-CA, G-CDCA and T-CDCA) increased in a time- and concentration-dependent manner (Figure 1 for the pooled donor hepatocyte lot, YZG) (Supplemental Figure 1 for the single donor hepatocyte lot, WWQ). The efflux of G-CA was 5.5, 15.7 and 27-fold higher at 1, 5 and 10 µM of CA compared to the efflux of endogenous G-CA whereas the efflux of T-CA was 2.8, 6.3 and 9.5-fold higher at 1, 5 and 10 µM of CA compared to the efflux of endogenous T-CA. Similarly, the efflux of G-CDCA was 9.5, 27.5 and 36.8-fold higher at 1, 5 and 10 µM of CDCA compared to the efflux of endogenous G-CDCA. While the efflux of T-CDCA was 3.3, 5.6 and 6.7-fold higher at 1, 5 and 10 µM of CDCA compared to the efflux of endogenous T-CDCA (Figure 1 for the pooled donor hepatocyte lot, YZG) (Supplemental Figure 1 for the single donor hepatocyte lot, WWQ). Interestingly, human hepatocytes generated more glycine-conjugated moieties than taurine-conjugated moieties. The amount of G-CA generated was 12.1 – 17.5-fold higher compared to T-CA while the amount of G-CDCA generated was 6.2 – 11.8-fold higher compared to T-CDCA.

Analysis of MRP3 and MRP4-mediated Transport of Bile Salts

Previous reports have indicated that MRP3 and MRP4 are involved in the transport of bile salts from hepatocytes into the systemic circulation(Zelcer et al., 2003;

DMD Fast Forward. Published on January 20, 2021 as DOI: 10.1124/dmd.120.000057
This article has not been copyedited and formatted. The final version may differ from this version.

Rius et al., 2006). To delineate the role of MRP3 and MRP4 in the transport of G-CA, T-CA, G-CDCA and T-CDCA, we tested the transport of these bile salts in MRP3 and MRP4 overexpressed membrane vesicles. MRP3 overexpressing vesicles showed 5.5- and 2.2-fold while MRP4 overexpressing vesicles showed 1.2-fold higher uptake of G-CA and T-CA, respectively in the presence of ATP compared to AMP (Figure 2A and B, supplemental table 6 and 7). On the other hand, MRP3 overexpressing vesicles showed 5.4- and 2.5-fold while MRP4 overexpressing vesicles showed 1.4- and 1.5-fold higher uptake of G-CDCA and T-CDCA, respectively in the presence of ATP compared to AMP (Figure 2A and B, supplemental table 6 and 7). As a positive control, the uptake of estradiol-17 β-glucuronide and DHEAS was 33.2-and 6.8-fold higher in the presence of ATP compared to AMP in MRP3 and MRP4 overexpressing vesicles, respectively (Supplemental Figure 2A and B respectively). We then measured the uptake of all 4 bile salts in human BSEP overexpressing vesicles for direct comparison with MRP3 and MRP4. In comparison to MRP3 and MRP4, BSEP transported all 4 bile salts very efficiently. The uptake of G-CA, T-CA, G-CDCA and T-CDCA was 41.7, 30.8, 11.6 and 11.7-fold higher in BSEP overexpressed vesicles in the presence of ATP compared to the uptake in the presence of AMP (Figure 2C, supplemental table 8). The uptake of TCA, a positive control substrate, was 34.9-fold higher in the presence of ATP in comparison to the uptake in the presence of AMP (Supplemental Figure 2C).

Protein Abundance of Major Hepatic Uptake and Efflux Transporters in SHH in Comparison to SCHH

We quantified 11 human liver transporter proteins including basolateral uptake transporters; OATP1B1, OATP1B3, OATP2B1, NTCP, OCT1, OAT2 and OAT7,

DMD Fast Forward. Published on January 20, 2021 as DOI: 10.1124/dmd.120.000057
This article has not been copyedited and formatted. The final version may differ from this version.

basolateral efflux transporter, MRP3 and canalicular efflux transporters, P-glycoprotein (P-gp), BSEP and MRP2 in SHH and SCHH (5^{th} day culture). The protein expression of MRP3, OAT7, BSEP and OCT1 was very similar between SHH and SCHH. Overall there was a good correlation (within 2-fold, r^2=0.84) in transporter protein expression between SHH and SCHH (Table 1).

Inhibition of G-CA and G-CDCA Efflux by Known Cholestatic Drugs in SHH

We investigated the effect of the 9 known cholestatic drugs including cyclosporin A, itraconazole, reserpine, troglitazone, bosentan, simvastatin, loratadine, valinomycin and lovastatin on the efflux of G-CA G-CDCA in pooled SHH. The reported half-maximal inhibitory concentration (IC_{50}) of these drugs in different systems is shown in Table 2. Cyclosporin A, troglitazone, simvastatin, loratadine, valinomycin and lovastatin inhibited G-CA efflux by 80% while itraconazole, reserpine and bosentan inhibited G-CA efflux by 50%, 60% and 44%, respectively. On the other hand, simvastatin, valinomycin, lovastatin, cyclosporin A, reserpine and troglitazone inhibited G-CDCA efflux by 79%, 62%, 65%, 47%, 53% and 49%, respectively while bosentan, loratidine and itraconazole showed only modest inhibition of G-CDCA efflux (23%, 24% and 15% respectively) (Figure 3A). Further, we determined a half-maximal inhibitory concentration (IC_{50}) of troglitazone for the inhibition of G-CA and G-CDCA efflux in pooled SHH. Human hepatocytes were incubated with CA and CDCA in the absence and presence of different concentrations of TGZ (0.05 – 50 µM) for 1h. Troglitazone inhibited G-CA and G-CDCA efflux with an IC_{50} of 9.9 ± 1.3 µM and 43.1 ± 2.6 µM, respectively (Figure 3B).

DMD Fast Forward. Published on January 20, 2021 as DOI: 10.1124/dmd.120.000057
This article has not been copyedited and formatted. The final version may differ from this version.

Uptake Analysis of CA and CDCA in SHH

Most cholestatic drugs are known to inhibit hepatic uptake transporters in addition to BSEP e.g. troglitazone is known to inhibit hepatic uptake transporters, OATPs(Chang et al., 2013) and NTCP(Yang et al., 2015) in addition to BSEP. Therefore, to delineate the implication of these uptake transporters in the inhibition of bile salt efflux we analyzed the uptake of CA and CDCA in human hepatocytes. The active uptake of CA and CDCA in SHH was assessed by incubating bile acids at 37 °C in the absence and presence of RFV (OATP inhibitor) and HBV peptide (NTCP inhibitor). The uptake of CA was reduced by 38% and 43% by RFV and HBV peptide respectively while the uptake of CDCA was only modestly reduced by 22% and 18% by both RFV and HBV peptide respectively (Figure 4). The total uptake of CDCA was found to be 5.6-fold higher compared to CA (Supplemental Table 4). For control, we measured the uptake of TCA and atorvastatin in pooled SHH. TCA uptake was measured in sodium-containing buffer (KHB) and sodium-free KHB buffer (sodium chloride was iso-osmotically replaced with choline chloride, BioreclamationIVT). The inhibition of TCA uptake by HBV peptide was measured in the presence of sodium-containing KHB buffer. NTCP-specific TCA uptake was determined by subtracting the uptake in sodium-free buffer from sodium-containing buffer. HBV peptide inhibited NTCP-mediated TCA uptake by 97% (Supplemental Figure 3A, $p<0.001$). Atorvastatin uptake was measured in the absence and presence of 20 µM RFV. The uptake of atorvastatin was significantly inhibited by RFV up to 61% (Supplemental Figure 3B, $p<0.001$).

DMD Fast Forward. Published on January 20, 2021 as DOI: 10.1124/dmd.120.000057
This article has not been copyedited and formatted. The final version may differ from this version.

DISCUSSION

Bile salt disposition is not well established in suspension human hepatocytes (SHH) due to the lack of information on the expression and function of bile salt export protein (BSEP). As described in the introduction, earlier studies by Bow D et. al. and Lundquist P et. al. were inconsistent in terms of plasma membrane expression of canalicular transporters, including BSEP, in suspension hepatocytes. Zhang J et. al. (2016) showed the transport function of BSEP in human, monkey, dog, rat and mouse suspension hepatocytes (Zhang et al., 2016) by using a novel method which involves *in situ* biosynthesis of bile salts from their precursor bile acids such as CA and CDCA. Their data showed dose- and time-dependent increase in the efflux of bile salts across species. In the present study, we used a similar approach to demonstrate BSEP activity in SHH. In addition, we also assessed protein abundance of BSEP in SHH in direct comparison with SCHH by targeted proteomics using the same lot of human hepatocytes. We also comprehensively investigated the contribution of BSEP to the biliary secretion of bile salts by directly comparing the transport of bile salts via BSEP

DMD Fast Forward. Published on January 20, 2021 as DOI: 10.1124/dmd.120.000057
This article has not been copyedited and formatted. The final version may differ from this version.

and basolateral MRPs and examining the effect of known BSEP inhibitors on bile salt efflux.

In the present study the efflux of conjugated bile salts was found to be concentration- and time-dependent. Glycine conjugation was favored over taurine conjugation as G-CA and G-CDCA levels were significantly higher than T-CA and T-CDCA in SHH. These data are consistent with data reported by Zhang J et. al. Further, G-CDCA was the most abundant bile salt generated in human hepatocytes which is also consistent with the clinical data (Luo et al., 2018). These data revealed that CA and CDCA are efficiently metabolized to their respective glycine- and taurine-conjugated salts which are subsequently transported out of hepatocytes. In the current study, vesicular transport data indicated that MRP3 does transport all 4 bile salts but MRP4 did not show transport of any bile salts at significant level (uptake ratio (ATP/AMP) <2). Although MRP3 is capable of transporting these bile salts the transport efficiency was significantly lower (2- to14-fold) compared to BSEP (Supplemental tables 6 and 8).

To further support the functional role of BSEP in bile salt transport in SHH, we quantitatively measured and compared the protein abundance of BSEP between SHH and SCHH. Interestingly, the membrane expression of BSEP in SHH was very similar to that in SCHH (Table 1). We examined BSEP protein expression in total membrane extract obtained from human hepatocytes which not only contains plasma membrane but also other intracellular membranes, therefore, it may not truly represent BSEP function. However, recent data by Kumar V et. al indicated that the plasma membrane as well as total protein expression of BSEP in SHH was comparable to SCHH although more than 50% of BSEP protein was found in intracellular space (Kumar et al., 2019).

DMD Fast Forward. Published on January 20, 2021 as DOI: 10.1124/dmd.120.000057
This article has not been copyedited and formatted. The final version may differ from this version.

Nevertheless, the fraction of BSEP protein present in the plasma membrane of human hepatocytes was functional as seen in the present study. The protein abundance of MRP3 was found to be relatively less compared to BSEP in both SHH and SCHH (1.6-fold and 2-fold less in SHH and SCHH, respectively). Although the protein abundance of MRP3 was evident in SHH and showed active transport of bile salts, its contribution to overall bile salt transport may be low under normal physiological conditions. Zheng H et. al. reported that MRP3-mediated GCA transport was low affinity and high capacity (K_m=248 µM) and it may play a significant role under cholestatic conditions when the intracellular G-CA concentration is high (Zeng et al., 2000). In this study we did not report the protein abundance of MRP4 as the protein level was below the level of detection due to its poor expression in human hepatocytes. This is not surprising as an earlier study by Kumar V et. al. could also not detect MRP4 protein in different human hepatocyte platforms (Kumar et al., 2019). We did not measure the protein abundance of OSTα/β in the present study as it is not known to play a significant role in bile salt transport under normal physiological conditions. Recently, Beaudoin J et. al. reported that the protein level of OSTα/β in SCHH was undetected under normal physiological conditions and the expression was only detectable after treatment with 100 µM CDCA which is known to induce MRP4 expression (Beaudoin et al., 2020a; Beaudoin et al., 2020b). Coincidentally, this study was done using the same lot of hepatocytes (WWQ) that was used in the present study for both bile salt transport and proteomics experiments (Beaudoin et al., 2020a). Furthermore, studies from Suga T et. al. and Beaudoin J et. al. showed that G-CA, T-CA, G-CDCA and T-CDCA are low affinity substrates of OSTα/β (Km > 700 µM for G-CA and TCA while Km > 1000 µM for G-

DMD Fast Forward. Published on January 20, 2021 as DOI: 10.1124/dmd.120.000057
This article has not been copyedited and formatted. The final version may differ from this version.

CDCA and T-CDCA) (Suga et al., 2019; Beaudoin et al., 2020a), therefore, OSTα/β may not recognize and transport these bile salts under normal conditions when intracellular concentrations of bile salts are low. However, it may contribute significantly to the efflux of these bile salts under cholestatic conditions when the intracellular concentrations of bile salts are high (Malinen et al., 2018; Beaudoin et al., 2020b). Overall, these data suggest that the efflux of T-CA and T-CDCA in suspension hepatocytes appears to be predominantly mediated by BSEP with little or no involvement of MRP3, MRP4 and OSTα/β. Since MRP3 showed significant transport of G-CA and G-CDCA in membrane vesicles (Supplemental Table 6) it is possible that it may play a major role in the efflux of these bile salts at the basolateral membrane of human hepatocytes when intracellular levels of these bile salts increase as a consequence of BSEP inhibition by cholestatic agents. Further studies such as the measurement of protein abundance of MRP3 and BSEP in MRP3- and BSEP-membrane vesicles is needed to quantitatively estimate the relative contribution of MRP3 and BSEP in the transport of G-CA and G-CDCA in SHH using Relative Expression Factor (REF) approach. Interestingly, the membrane abundance of NTCP and OCT1 was found to be 3-fold and 2-fold lower, respectively compared to the data available in literature (Schaefer et al., 2012; Kumar et al., 2019). This discrepancy cannot be explained at this time.

To further confirm the functional expression of BSEP in SHH we assessed the inhibitory effect of known cholestatic drugs on BSEP function in SHH. Most of the drugs showed substrate (G-CA or G-CDCA) dependent inhibitory effect on BSEP function. The majority of the inhibitors consistently indicated higher potency on the inhibition of G-CA

DMD Fast Forward. Published on January 20, 2021 as DOI: 10.1124/dmd.120.000057
This article has not been copyedited and formatted. The final version may differ from this version.

efflux compared to G-CDCA efflux. Next, we determined IC_{50} of troglitazone on the inhibition G-CA and G-CDCA efflux. We selected troglitazone for the following reasons; it showed significant differential effects on the inhibition of G-CA and G-CDCA efflux (3.6-fold); its cholestatic effects are well studied and known to involve BSEP inhibition and its interaction with other hepatic transporters are well characterized. As expected troglitazone showed higher potency (4-fold) for BSEP inhibition using G-CA compared to G-CDCA as a substrate. This differential inhibitory effect was also evident in a previous study by Yucha R et. al. where troglitazone inhibited GCA and GCDCA efflux with IC_{50}'s of 1.2 and 22.6 M, respectively in suspension human hepatocytes (Yucha et al., 2017) (Table 2). Based on these data, we hypothesized that the observed discrepancy in the potency of troglitazone is related to the differential disposition of precursor bile acids, CA and CDCA. To test this hypothesis, we examined the uptake of both CA and CDCA in human hepatocytes. Previously, CA has been shown to be a substrate of both OATPs (Suga et al., 2017) and NTCP (Kouzuki et al., 1998) while CDCA is a substrate of OATPs (Yamaguchi et al., 2006) but not NTCP (Jani et al., 2018). Our data indicated that CA but not CDCA is a substrate of OATPs and NTCP as the uptake of CA and not CDCA was significantly inhibited by 20 µM RFV (selectively inhibiting OATP1B1, OATP1B3 and OATP2B1) and 0.1 µM HBV peptide (selectively inhibiting NTCP) (Bi et al., 2019) in SHH (Figure 4). These data also indicated that, in addition to the active uptake via NTCP and OATPs, there is significant contribution by passive diffusion (57%) to the hepatic uptake of CA, while the uptake of CDCA was primarily by passive diffusion (82%) (Supplemental Table 4). Furthermore, CA appears to have low permeability while CDCA appears to have moderate permeability in MDCKII

DMD Fast Forward. Published on January 20, 2021 as DOI: 10.1124/dmd.120.000057
This article has not been copyedited and formatted. The final version may differ from this version.

cells (Supplemental Table 5). Previously, MDCK cell model has been proposed as a surrogate for human hepatocytes for permeability assessment as the apparent permeabilities of some anionic drugs (anionic at pH 7.4) in MDCK cells strongly correlated with the apparent permeabilities in human hepatocytes(Li et al., 2014). Therefore, the permeability of bile acids/salts (anionic at pH 7.4) assessed in this study should be similar between MDCK and human hepatocytes. Collectively, these data confirmed that both active uptake (via NTCP and OATPs) and passive diffusion play an important role in the liver uptake of CA while CDCA, being moderately permeable, may not require uptake transporters as passive diffusion can play a major role in its liver uptake. In addition to BSEP, troglitazone is also an inhibitor of NTCP, OATPs (Gui et al., 2008; Gui et al., 2009; Yang et al., 2015), MRP3 (IC_{50}: 31 µM) and MRP4 (IC_{50}: 61 µM) (Morgan et al., 2013). However, TGZ is not an inhibitor of OSTα/β as indicated by Malinen MM et. al. (IC_{50} value >200 µM) (Malinen et al., 2018).

Thus, inhibition of G-CA efflux by troglitazone is the outcome of BSEP inhibition, uptake inhibition of CA (precursor bile acid), and probably MRP3/MRP4 inhibition. On the contrary, inhibition of G-CDCA efflux by troglitazone is attributed to only BSEP inhibition as CDCA (precursor bile acid) is not transported by hepatic uptake transporters and G-CDCA is relatively weak substrate of MRP3, MRP4 (Figure 2A-B) and OSTα/β (Beaudoin et al., 2020a). Therefore, G-CDCA can serve as a relevant substrate to reliably assess BSEP inhibition by cholestatic drugs in SHH (Figure 5). Further studies are warranted to assess BSEP inhibition by known cholestatic and DILI causing drugs using G-CDCA as a probe substrate in SHH.

DMD Fast Forward. Published on January 20, 2021 as DOI: 10.1124/dmd.120.000057
This article has not been copyedited and formatted. The final version may differ from this version.

In summary, BSEP transport function was evident in SHH as shown by the efflux of G-CA, T-CA, G-CDCA and T-CDCA. BSEP protein abundance was found to be similar between SHH and SCHH. Furthermore, MRP3 and MRP4 may not play significant role in the transport of these bile salts and finally, the cholestatic drugs (known to inhibit BSEP) significantly inhibited BSEP-mediated G-CA and G-CDCA efflux that further confirmed the functional expression of BSEP in SHH. These data clearly indicated the potential utility of SHH in the mechanistic understanding of bile salt disposition and in the assessment of potential inhibitory effect of drugs on BSEP inhibition.

Authorship Contributions

Participated in research design: Chothe, Hariparsad.

Conducted experiments: Chothe, Pemberton.

Performed data analysis: Chothe, Hariparsad.

Wrote or contributed to the writing of the manuscript: Chothe, Hariparsad.

DMD Fast Forward. Published on January 20, 2021 as DOI: 10.1124/dmd.120.000057
This article has not been copyedited and formatted. The final version may differ from this version.

References

Beaudoin JJ, Bezencon J, Sjostedt N, Fallon JK, and Brouwer KLR (2020a) Role of Organic Solute Transporter Alpha/Beta in Hepatotoxic Bile Acid Transport and Drug Interactions. *Toxicol Sci*.

Beaudoin JJ, Brouwer KLR, and Malinen MM (2020b) Novel insights into the organic solute transporter alpha/beta, OSTalpha/beta: From the bench to the bedside. *Pharmacol Ther***:**107542.

Bi YA, Costales C, Mathialagan S, West M, Eatemadpour S, Lazzaro S, Tylaska L, Scialis R, Zhang H, Umland J, Kimoto E, Tess DA, Feng B, Tremaine LM, Varma MVS, and Rodrigues AD (2019) Quantitative Contribution of Six Major Transporters to the Hepatic Uptake of Drugs: "SLC-Phenotyping" Using Primary Human Hepatocytes. *J Pharmacol Exp Ther* **370:**72-83.

Bow DA, Perry JL, Miller DS, Pritchard JB, and Brouwer KL (2008) Localization of P-gp (Abcb1) and Mrp2 (Abcc2) in freshly isolated rat hepatocytes. *Drug Metab Dispos* **36:**198-202.

Chang JH, Plise E, Cheong J, Ho Q, and Lin M (2013) Evaluating the in vitro inhibition of UGT1A1, OATP1B1, OATP1B3, MRP2, and BSEP in predicting drug-induced hyperbilirubinemia. *Mol Pharm* **10:**3067-3075.

Chiba M, Ishii Y, and Sugiyama Y (2009) Prediction of hepatic clearance in human from in vitro data for successful drug development. *AAPS J* **11:**262-276.

Chothe PP, Wu SP, Ye Z, and Hariparsad N (2018) Assessment of Transporter-Mediated and Passive Hepatic Uptake Clearance Using Rifamycin-SV as a Pan-Inhibitor of Active Uptake. *Mol Pharm* **15:**4677-4688.

Gomez-Lechon MJ, Donato MT, Castell JV, and Jover R (2004) Human hepatocytes in primary culture: the choice to investigate drug metabolism in man. *Curr Drug Metab* **5:**443-462.

Gui C, Miao Y, Thompson L, Wahlgren B, Mock M, Stieger B, and Hagenbuch B (2008) Effect of pregnane X receptor ligands on transport mediated by human OATP1B1 and OATP1B3. *Eur J Pharmacol* **584:**57-65.

Gui C, Wahlgren B, Lushington GH, and Hagenbuch B (2009) Identification, Ki determination and CoMFA analysis of nuclear receptor ligands as competitive inhibitors of OATP1B1-mediated estradiol-17beta-glucuronide transport. *Pharmacol Res* **60:**50-56.

Jani M, Beery E, Heslop T, Toth B, Jagota B, Kis E, Kevin Park B, Krajcsi P, and Weaver RJ (2018) Kinetic characterization of bile salt transport by human NTCP (SLC10A1). *Toxicol In Vitro* **46:**189-193.

Keemink J, Deferm N, De Bruyn T, Augustijns P, Bouillon T, and Annaert P (2018) Effect of Cryopreservation on Enzyme and Transporter Activities in Suspended and Sandwich Cultured Rat Hepatocytes. *AAPS J* **20:**33.

Khatri R, Fallon JK, Rementer RJB, Kulick NT, Lee CR, and Smith PC (2019) Targeted quantitative proteomic analysis of drug metabolizing enzymes and transporters by nano LC-MS/MS in the sandwich cultured human hepatocyte model. *J Pharmacol Toxicol Methods* **98:**106590.

Kis E, Ioja E, Nagy T, Szente L, Heredi-Szabo K, and Krajcsi P (2009) Effect of membrane cholesterol on BSEP/Bsep activity: species specificity studies for substrates and inhibitors. *Drug Metab Dispos* **37:**1878-1886.

Konig A, Doring B, Mohr C, Geipel A, Geyer J, and Glebe D (2014) Kinetics of the bile acid transporter and hepatitis B virus receptor Na+/taurocholate cotransporting polypeptide (NTCP) in hepatocytes. *J Hepatol* **61:**867-875.

Kouzuki H, Suzuki H, Ito K, Ohashi R, and Sugiyama Y (1998) Contribution of sodium taurocholate co-transporting polypeptide to the uptake of its possible substrates into rat hepatocytes. *J Pharmacol Exp Ther* **286:**1043-1050.

Kumar V, Salphati L, Hop C, Xiao G, Lai Y, Mathias A, Chu X, Humphreys WG, Liao M, Heyward S, and Unadkat JD (2019) A Comparison of Total and Plasma Membrane Abundance of Transporters in Suspended, Plated, Sandwich-Cultured Human Hepatocytes Versus Human Liver Tissue Using Quantitative Targeted Proteomics and Cell Surface Biotinylation. *Drug Metab Dispos* **47:**350-357.

Lempers VJ, van den Heuvel JJ, Russel FG, Aarnoutse RE, Burger DM, Bruggemann RJ, and Koenderink JB (2016) Inhibitory Potential of Antifungal Drugs on ATP-Binding Cassette Transporters P-Glycoprotein, MRP1 to MRP5, BCRP, and BSEP. *Antimicrob Agents Chemother* **60:**3372-3379.

Li M, Yuan H, Li N, Song G, Zheng Y, Baratta M, Hua F, Thurston A, Wang J, and Lai Y (2008) Identification of interspecies difference in efflux transporters of hepatocytes from dog, rat, monkey and human. *Eur J Pharm Sci* **35:**114-126.

Li N, Palandra J, Nemirovskiy OV, and Lai Y (2009a) LC-MS/MS mediated absolute quantification and comparison of bile salt export pump and breast cancer resistance protein in livers and hepatocytes across species. *Anal Chem* **81:**2251-2259.

Li N, Zhang Y, Hua F, and Lai Y (2009b) Absolute difference of hepatobiliary transporter multidrug resistance-associated protein (MRP2/Mrp2) in liver tissues and isolated hepatocytes from rat, dog, monkey, and human. *Drug Metab Dispos* **37:**66-73.

Li R, Bi YA, Lai Y, Sugano K, Steyn SJ, Trapa PE, and Di L (2014) Permeability comparison between hepatocyte and low efflux MDCKII cell monolayer. *AAPS J* **16:**802-809.

Lundquist P, Englund G, Skogastierna C, Loof J, Johansson J, Hoogstraate J, Afzelius L, and Andersson TB (2014) Functional ATP-binding cassette drug efflux transporters in isolated human and rat hepatocytes significantly affect assessment of drug disposition. *Drug Metab Dispos* **42:**448-458.

Luo L, Aubrecht J, Li D, Warner RL, Johnson KJ, Kenny J, and Colangelo JL (2018) Assessment of serum bile acid profiles as biomarkers of liver injury and liver disease in humans. *PLoS One* **13:**e0193824.

Malinen MM, Ali I, Bezencon J, Beaudoin JJ, and Brouwer KLR (2018) Organic solute transporter OSTalpha/beta is overexpressed in nonalcoholic steatohepatitis and modulated by drugs associated with liver injury. *Am J Physiol Gastrointest Liver Physiol* **314:**G597-G609.

Moore A, Chothe PP, Tsao H, and Hariparsad N (2016) Evaluation of the Interplay between Uptake Transport and CYP3A4 Induction in Micropatterned Cocultured Hepatocytes. *Drug Metab Dispos* **44:**1910-1919.

Morgan RE, van Staden CJ, Chen Y, Kalyanaraman N, Kalanzi J, Dunn RT, 2nd, Afshari CA, and Hamadeh HK (2013) A multifactorial approach to hepatobiliary transporter assessment enables improved therapeutic compound development. *Toxicol Sci* **136:**216-241.

Richert L, Liguori MJ, Abadie C, Heyd B, Mantion G, Halkic N, and Waring JF (2006) Gene expression in human hepatocytes in suspension after isolation is similar to the liver of origin, is not affected by hepatocyte cold storage and cryopreservation, but is strongly changed after hepatocyte plating. *Drug Metab Dispos* **34:**870-879.

Rius M, Hummel-Eisenbeiss J, Hofmann AF, and Keppler D (2006) Substrate specificity of human ABCC4 (MRP4)-mediated cotransport of bile acids and reduced glutathione. *Am J Physiol Gastrointest Liver Physiol* **290:**G640-649.

Schaefer O, Ohtsuki S, Kawakami H, Inoue T, Liehner S, Saito A, Sakamoto A, Ishiguro N, Matsumaru T, Terasaki T, and Ebner T (2012) Absolute quantification and differential expression of drug transporters, cytochrome P450 enzymes, and UDP-glucuronosyltransferases in cultured primary human hepatocytes. *Drug Metab Dispos* **40:**93-103.

Soars MG, Grime K, Sproston JL, Webborn PJ, and Riley RJ (2007) Use of hepatocytes to assess the contribution of hepatic uptake to clearance in vivo. *Drug Metab Dispos* **35:**859-865.

Suga T, Yamaguchi H, Ogura J, and Mano N (2019) Characterization of conjugated and unconjugated bile acid transport via human organic solute transporter alpha/beta. *Biochim Biophys Acta Biomembr* **1861:**1023-1029.

Suga T, Yamaguchi H, Sato T, Maekawa M, Goto J, and Mano N (2017) Preference of Conjugated Bile Acids over Unconjugated Bile Acids as Substrates for OATP1B1 and OATP1B3. *PLoS One* **12:**e0169719.

Wang EJ, Casciano CN, Clement RP, and Johnson WW (2003) Fluorescent substrates of sister-P-glycoprotein (BSEP) evaluated as markers of active transport and inhibition: evidence for contingent unequal binding sites. *Pharm Res* **20:**537-544.

Yamaguchi H, Okada M, Akitaya S, Ohara H, Mikkaichi T, Ishikawa H, Sato M, Matsuura M, Saga T, Unno M, Abe T, Mano N, Hishinuma T, and Goto J (2006) Transport of fluorescent chenodeoxycholic acid via the human organic anion transporters OATP1B1 and OATP1B3. *J Lipid Res* **47:**1196-1202.

Yan H, Peng B, Liu Y, Xu G, He W, Ren B, Jing Z, Sui J, and Li W (2014) Viral entry of hepatitis B and D viruses and bile salts transportation share common molecular determinants on sodium taurocholate cotransporting polypeptide. *J Virol* **88:**3273-3284.

Yang K, Guo C, Woodhead JL, St Claire RL, 3rd, Watkins PB, Siler SQ, Howell BA, and Brouwer KLR (2016) Sandwich-Cultured Hepatocytes as a Tool to Study Drug Disposition and Drug-Induced Liver Injury. *J Pharm Sci* **105:**443-459.

Yang K, Pfeifer ND, Kock K, and Brouwer KL (2015) Species differences in hepatobiliary disposition of taurocholic acid in human and rat sandwich-cultured hepatocytes: implications for drug-induced liver injury. *J Pharmacol Exp Ther* **353:**415-423.

Yucha RW, He K, Shi Q, Cai L, Nakashita Y, Xia CQ, and Liao M (2017) In Vitro Drug-Induced Liver Injury Prediction: Criteria Optimization of Efflux Transporter IC50 and Physicochemical Properties. *Toxicol Sci* **157:**487-499.

Zelcer N, Saeki T, Bot I, Kuil A, and Borst P (2003) Transport of bile acids in multidrug-resistance-protein 3-overexpressing cells co-transfected with the ileal Na+-dependent bile-acid transporter. *Biochem J* **369:**23-30.

Zeng H, Liu G, Rea PA, and Kruh GD (2000) Transport of amphipathic anions by human multidrug resistance protein 3. *Cancer Res* **60:**4779-4784.

Zhang J, He K, Cai L, Chen YC, Yang Y, Shi Q, Woolf TF, Ge W, Guo L, Borlak J, and Tong W (2016) Inhibition of bile salt transport by drugs associated with liver injury in primary hepatocytes from human, monkey, dog, rat, and mouse. *Chem Biol Interact* **255:**45-54.

Zhao P (2008) The use of hepatocytes in evaluating time-dependent inactivation of P450 in vivo. *Expert Opin Drug Metab Toxicol* **4:**151-164.

Footnote

Paresh P. Chothe declares that he holds common stocks in Takeda Pharmaceutical Company Limited and, Rachel Pemberton and Niresh Hariparsad hold stocks in Vertex Pharmaceuticals Inc. This work received no external funding.

DMD Fast Forward. Published on January 20, 2021 as DOI: 10.1124/dmd.120.000057
This article has not been copyedited and formatted. The final version may differ from this version.

Figure legends

Figure 1. Efflux of Glycine- and Taurine-conjugated CA and CDCA in Pooled SHH (YZG). Cells were incubated with CA and CDCA at 1, 5 and 10 µM. Efflux of (A) G-CA, (B) TCA, (C) G-CDCA and (D) T-CDCA was measured at 15, 30, 60 and 120 minutes. For control experiment cells were incubated with vehicle (DMSO <0.1%). The experiment was done in triplicate (n=3).

Figure 2. Uptake Analysis of G-CA, T-CA, G-CDCA and T-CDCA in human MRP3, MRP4 and BSEP Overexpressed Membrane Vesicles. Uptake of G-CA, T-CA, G-CDCA and T-CDCA at 1 µM concentration was measured in the presence of AMP and ATP with and without MK571 (150 µM) in (A) MRP3, (B) MRP4 overexpressed membrane vesicles. (C) Uptake of G-CA, T-CA, G-CDCA and T-CDCA at 1 µM concentration was measured in the presence of AMP and ATP with and without CsA (10 µM) in BSEP overexpressed membrane vesicles. The experiment was done in triplicate (n=3). ** $p \leq 0.005$, *** $p < 0.001$.

DMD Fast Forward. Published on January 20, 2021 as DOI: 10.1124/dmd.120.000057
This article has not been copyedited and formatted. The final version may differ from this version.

Figure 3. Inhibition of G-CA and G-CDCA Efflux by cholestatic drugs in Pooled SHH. A) Hepatocytes were incubated with 5 µM CA and CDCA in the absence and presence of cyclosporin A (10 µM), itraconazole (5 µM), reserpine (10 µM), troglitazone (50 µM), bosentan (100 µM), simvastatin (100 µM), loratadine (100 µM), valinomycin (5 µM) and lovastatin (100 µM) for 1 h. The efflux of G-CA and G-CDCA was determined by quantifying G-CA and G-CDCA in incubation medium by LC-MS/MS. B) Hepatocytes were incubated with 5 µM CA and CDCA in the absence and presence of different concentrations of troglitazone (0.1 - 50 µM) for 1h. G-CA and G-CDCA was quantified in incubation medium by LC-MS/MS to measure the efflux. The rate of efflux of G-CA and G-CDCA in the presence of different concentrations of troglitazone was determined as a percent of control (DMSO). The experiment was done in triplicate (n=3).

Figure 4. Uptake Analysis of CA and CDCA in SHH. Uptake of 2 µM CA and CDCA was measured in the absence and presence of RFV (20 µM, OATP inhibitor) and HBV peptide (0.1 µM, NTCP inhibitor) in pooled suspension human hepatocytes (YJG). The data is presented as a percent of DMSO control. Horizontal dotted line indicates 50% of control. The experiment was done in triplicate (n=3). ** p value 0.005

DMD Fast Forward. Published on January 20, 2021 as DOI: 10.1124/dmd.120.000057
This article has not been copyedited and formatted. The final version may differ from this version.

Table 1: Protein Abundance of Liver Uptake and Efflux Transporters in SHH and Sandwich Cultured Human Hepatocytes

Protein	Peptide Sequence	pmol/mg membrane protein				Expression Ratio (suspension/SCHH)
		Suspension (n=4)	SD	SCHH (n=4)	SD	
P-gp	I_{368}IDNKPSIDSYSK$_{380}$	0.45	0.07	0.66	0.17	0.68
MRP2	Y_{514}FAWEPSFR$_{522}$	1.0	0.75	1.7	0.93	0.59
MRP3	G_{654}ALVAVVGPVGCGK$_{667}$	0.42	0.53	0.41	0.63	1.02
OATP1B1	N_{321}VTGFFQSFK$_{330}$	4.5	0.35	2.9	0.57	1.55
OATP1B3	I_{615}YNSVFFGR$_{623}$	0.48	0.58	0.22	0.43	2.18
OATP2B1	Y_{641}YNNDLLR$_{648}$	1.6	0.39	0.85	0.59	1.88
OAT2	N_{20}VALLALPR$_{28}$	0.35	0.29	0.16	0.11	2.19
OAT7	D_{313}TLTLEILK$_{321}$	1.5	0.10	1.2	0.30	1.25

DMD Fast Forward. Published on January 20, 2021 as DOI: 10.1124/dmd.120.000057
This article has not been copyedited and formatted. The final version may differ from this version.

BSEP	S_{462}TALQLIQR$_{470}$	0.67	0.18	0.80	0.12	0.84
NTCP	G_{144}IYDGDLK$_{151}$	0.10	0.14	0.20	0.13	0.5
OCT1	L_{330}SPSFADLFR$_{339}$	0.33	0.08	0.40	0.30	0.83
NaK ATPase	V_{213}DNSSLTGESEPQTR$_{227}$	9.0	0.24	10.4	0.39	0.87
GammaGTP	L_{156}FQPSIQLAR$_{165}$	1.4	0.30	3.7	1.0	0.39

Table 2: Summary of Compounds Known to Inhibit BSEP-mediated Bile Salt Transport.

Compound	Test system	Substrate (μM)	IC_{50} (μM)	Reference
Cyclosporin A	Sf9 vesicles	GCA (2)	0.93, 1.2	**(Kis et al., 2009; Yucha et al., 2017)**
		TCA (2)	18.9, 0.5, 2.2	(Kis et al., 2009; Morgan et al., 2013; Yucha et al., 2017)
		GCDCA (2)	9.4	(Kis et al., 2009)
		TCDCA (2)	0.94	(Kis et al., 2009)
	SHH*	GCA$	0.1, 0.27	(Zhang et al., 2016; Yucha et al., 2017)
		TCA$	0.3	(Yucha et al., 2017)
		GCDCA#	22.8	(Yucha et al., 2017)
		TCDCA#	100	(Yucha et al., 2017)
	SK-E2 cells	H_2FDA (0.2)	7.8	(Wang et al., 2003)
Itraconazole	Sf9 vesicles	TCA (2)	18, 22.1	(Morgan et al., 2013; Yucha et al., 2017)
		GCA (2)	4.8	(Yucha et al., 2017)
	HEK-293 vesicles	TCA (0.1)	3	(Lempers et al., 2016)
	SHH*	GCA$	100	(Yucha et al., 2017)
		TCA$	100	(Yucha et al., 2017)
		GCDCA#	100	(Yucha et al., 2017)
		TCDCA#	100	(Yucha et al., 2017)
Reserpine	Sf9 vesicles	TCA (2)	2.8, 8.4	(Kis et al., 2009; Morgan et al., 2013)
	SK-E2 cells	H_2FDA (0.2)	10.2	(Wang et al., 2003)
Troglitazone	Sf9 vesicles	TCA (2)	9.5, 3	(Kis et al., 2009; Morgan et al., 2013)
		GCA (2)	16	(Yucha et al., 2017)
	SHH*	GCA$	0.48, 1.2	(Zhang et al., 2016; Yucha et al., 2017)
		TCA$	0.6	(Yucha et al., 2017)
		GCDCA#	5.9	(Yucha et al., 2017)
		TCDCA#	26.6	(Yucha et al., 2017)
	SK-E2 cells	H_2FDA (0.2)	66.4	(Wang et al., 2003)
Bosentan	Sf9 vesicles	TCA (2)	23, 25.4	(Morgan et al., 2013; Yucha et al., 2017)
		GCA (2)	14.4	(Yucha et al., 2017)
	SHH*	GCA$	9.2, 26.5	(Zhang et al., 2016; Yucha et al., 2017)
		TCA$	26.6	(Yucha et al., 2017)
		GCDCA#	100	(Yucha et al., 2017)

		TCDCA[#]	100	(Yucha et al., 2017)
Simvastatin	Sf9 vesicles	TCA (2)	24.7	(Morgan et al., 2013)
Loratadine	Sf9 vesicles	TCA (2)	12	(Morgan et al., 2013)
Valinomycin	Sf9 vesicles SK-E2 cells	TCA (2) H_2FDA (0.2)	1.56 7.2	(Morgan et al., 2013) (Wang et al., 2003)
Lovastatin	Sf9 vesicles SHH[*]	TCA (2) GCA[$]	19.3 1.7	(Morgan et al., 2013) (Zhang et al., 2016)

[*] suspension human hepatocytes

[$] suspension human hepatocytes were incubated with cholic acid (10 µM) and the efflux of GCA or TCA was measured.

[#] suspension human hepatocytes were incubated with chenodeoxycholic acid (10 µM) and the efflux of GCDCA or TCDCA was measured.

DMD Fast Forward. Published on January 20, 2021 as DOI: 10.1124/dmd.120.000057
This article has not been copyedited and formatted. The final version may differ from this version.

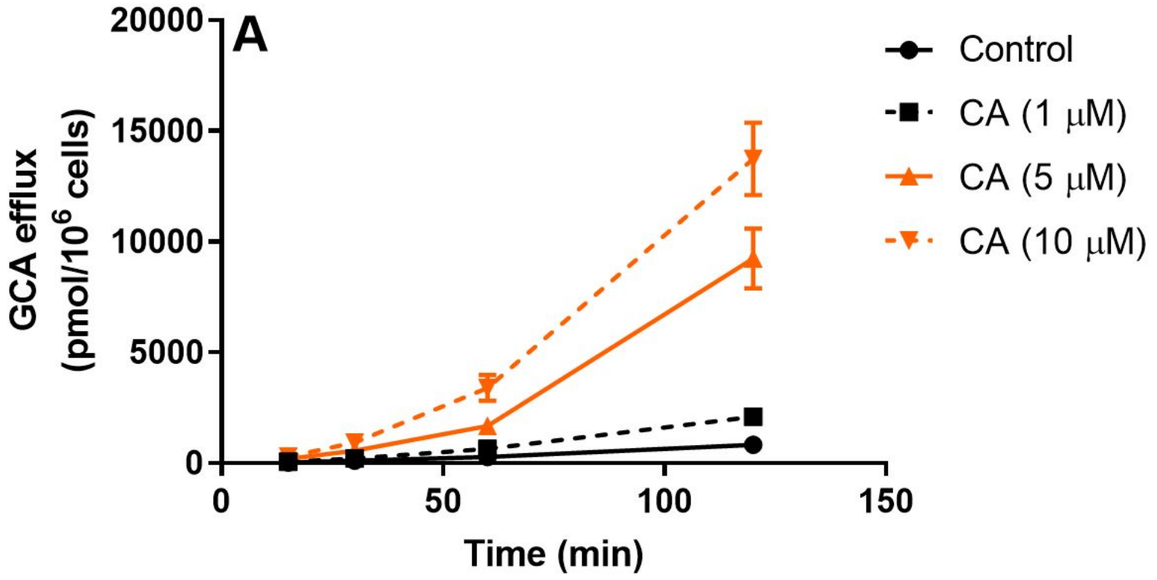

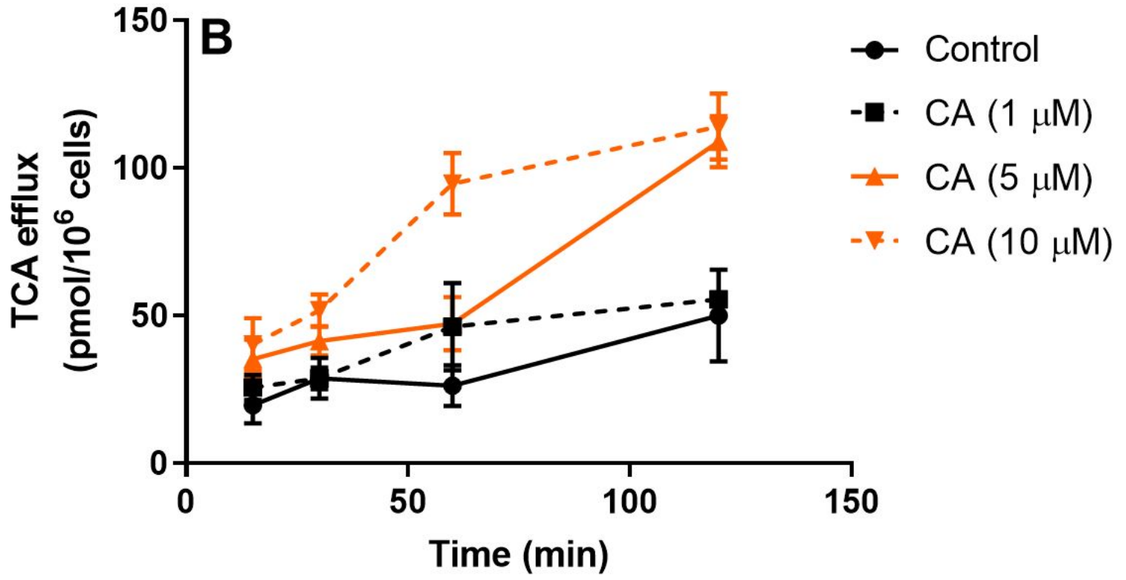

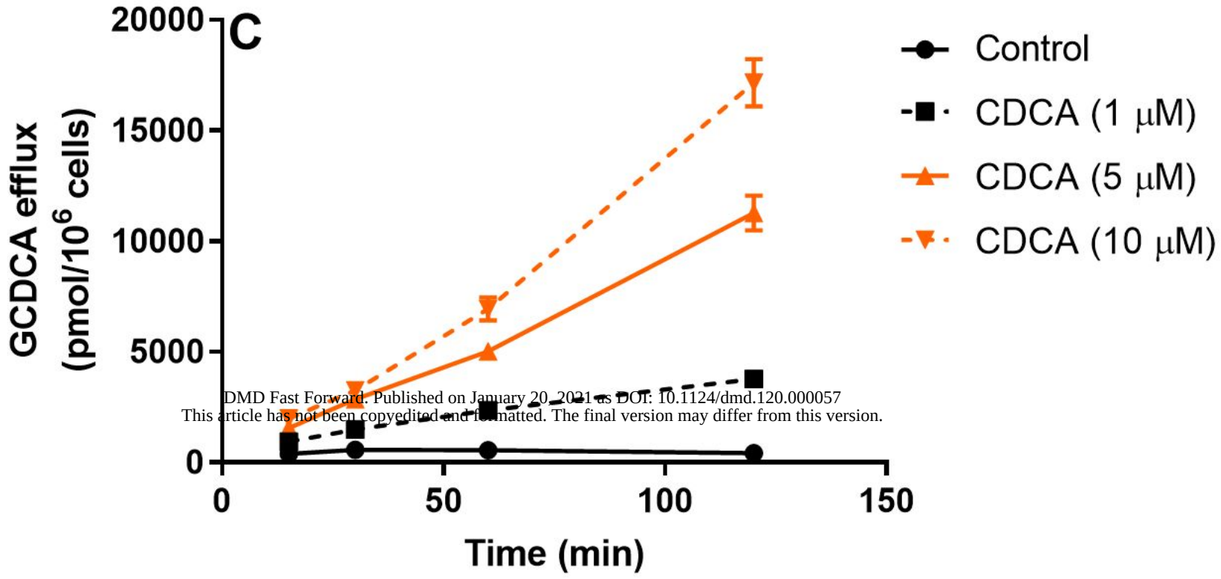

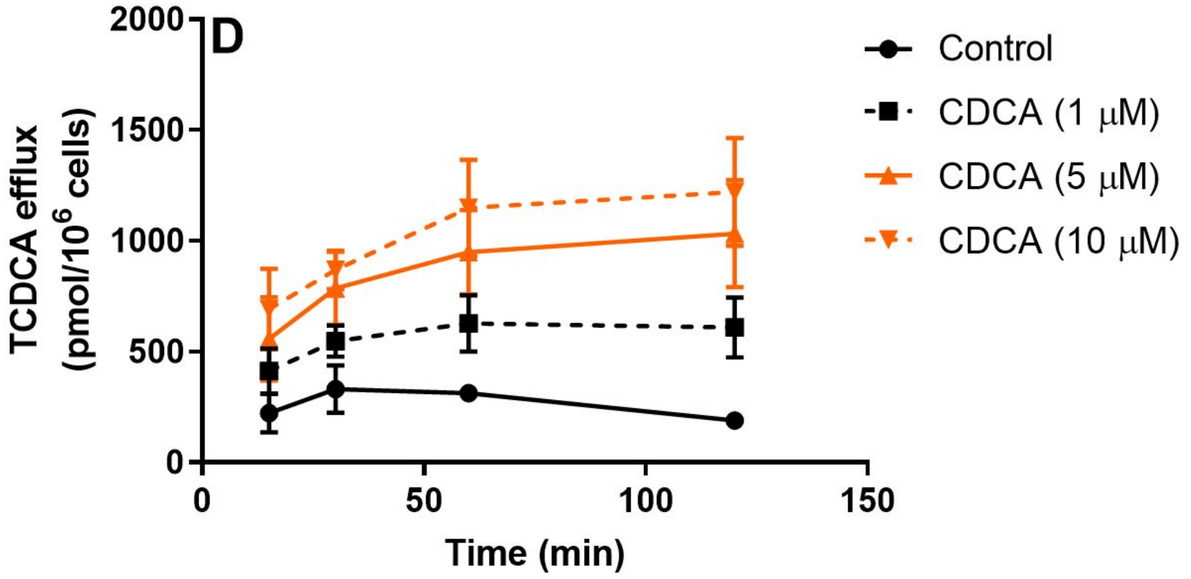

Figure 1

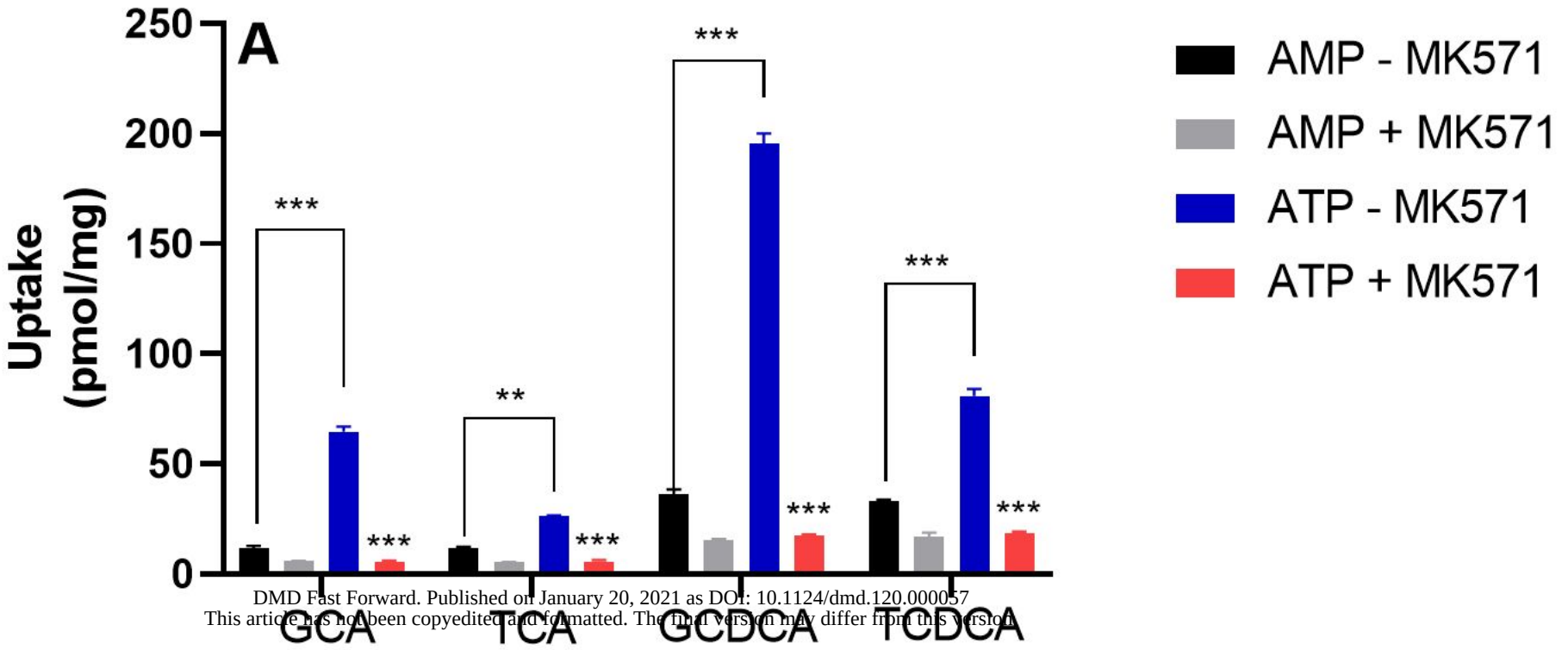

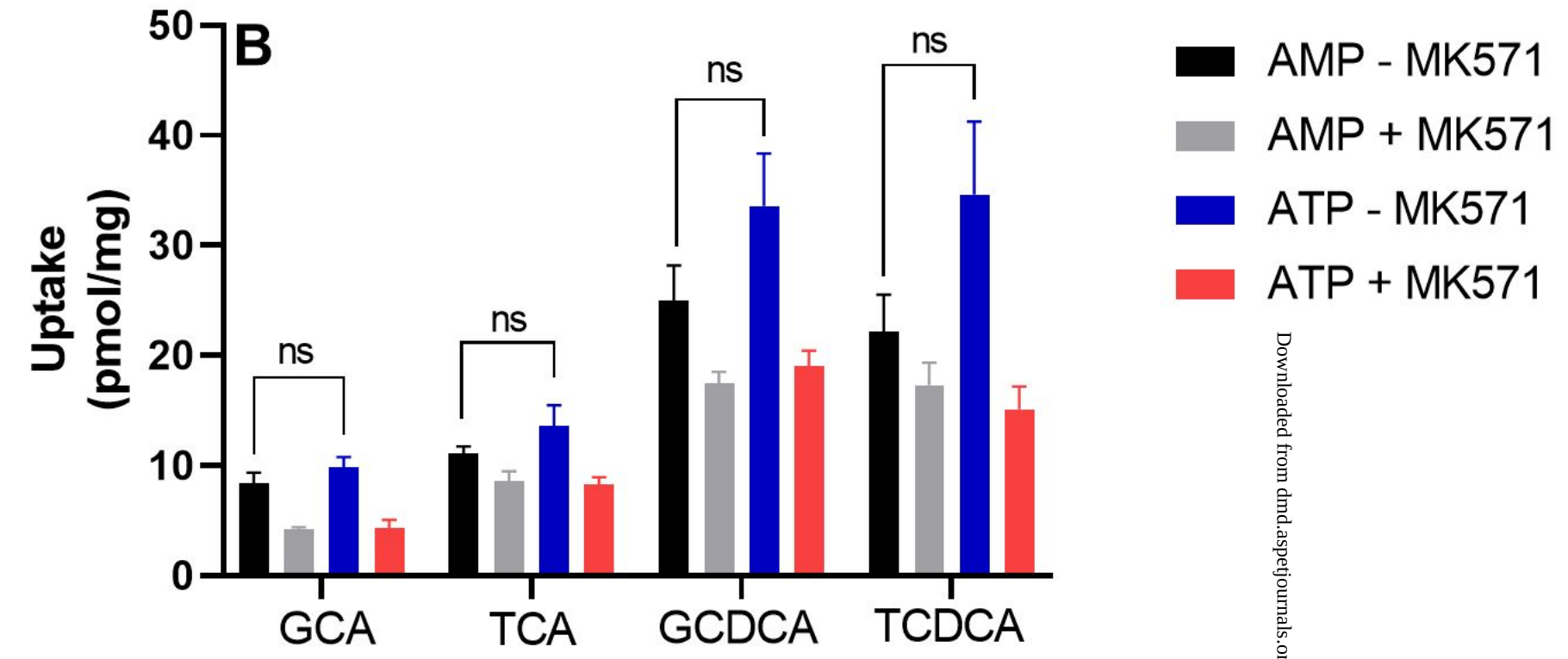

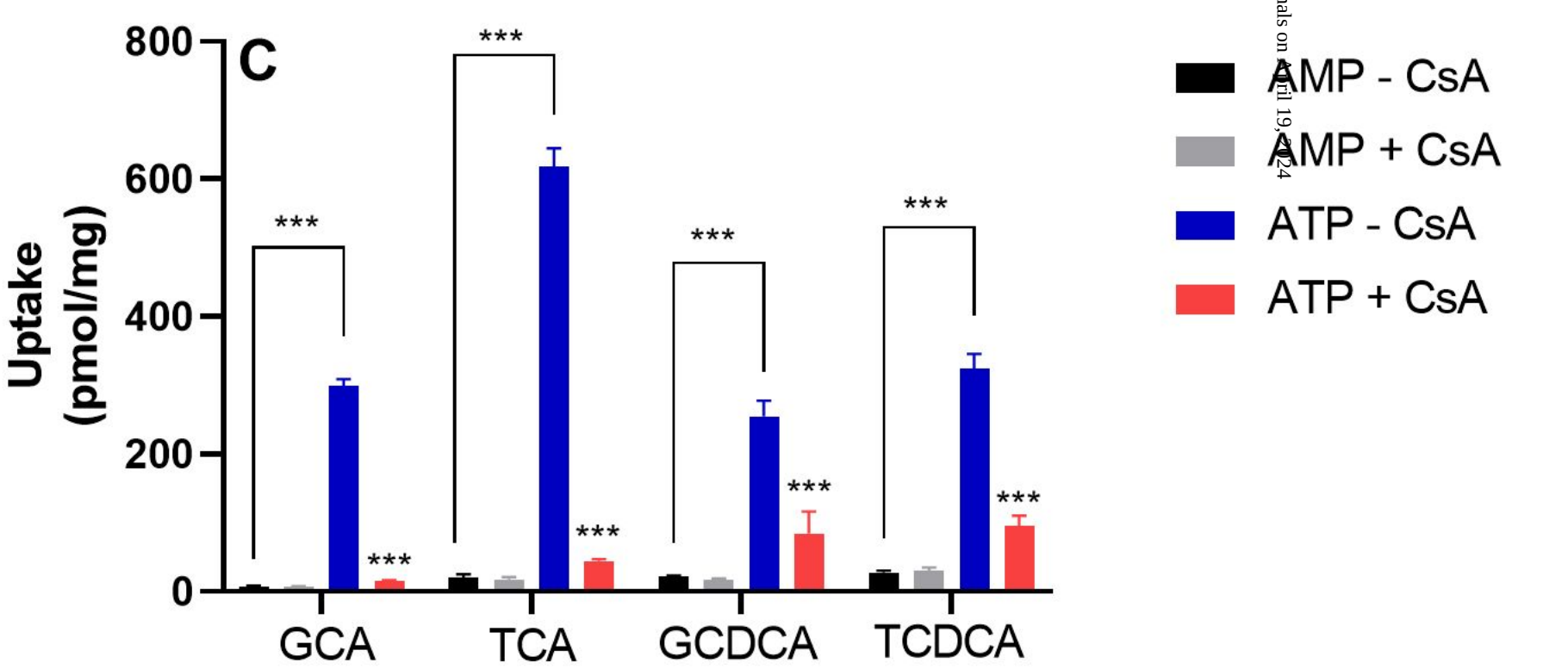

Figure 2

DMD Fast Forward. Published on January 20, 2021 as DOI: 10.1124/dmd.120.000057
This article has not been copyedited and formatted. The final version may differ from this version.

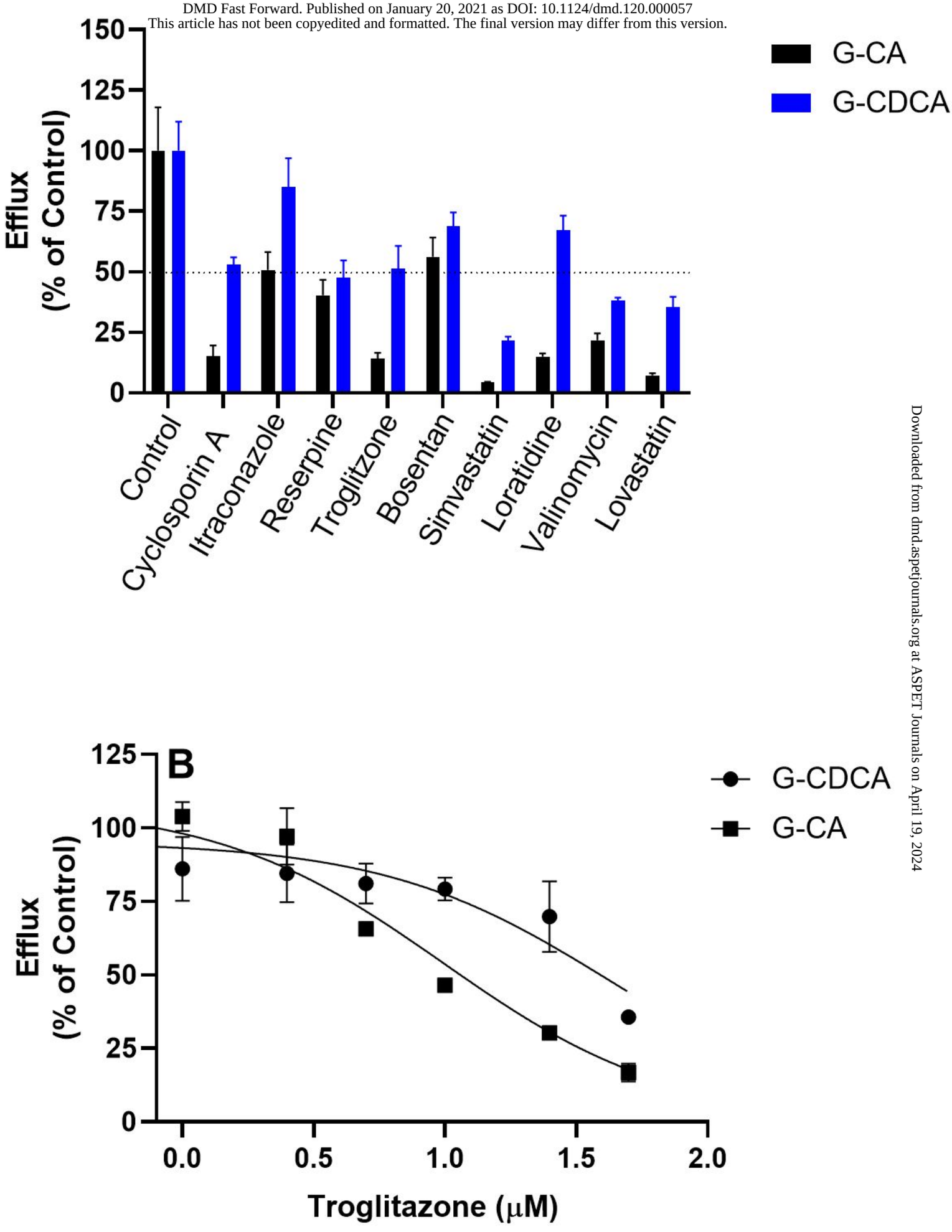

Figure 3

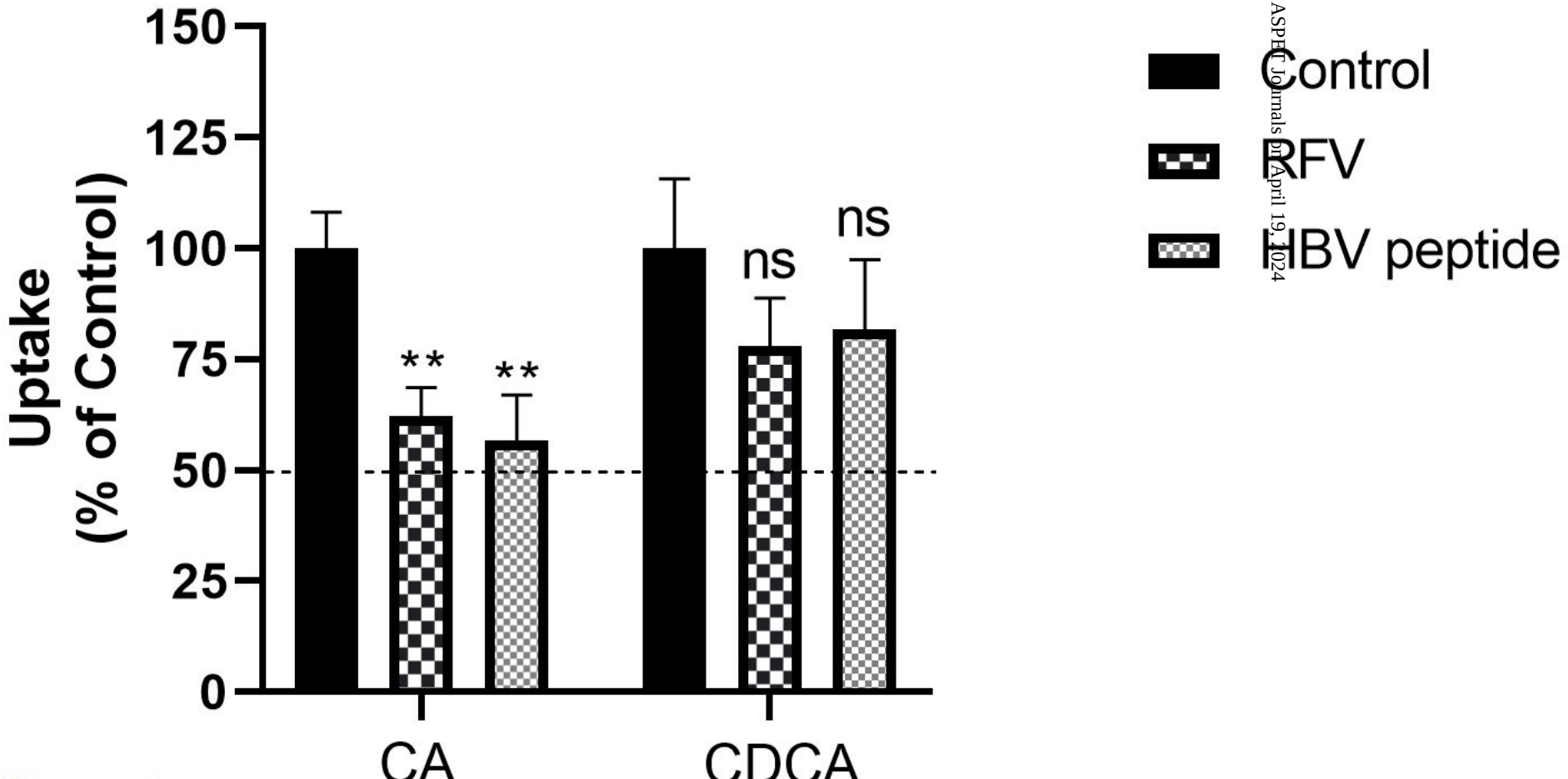

Figure 4

Function and Expression of Bile Salt Export Pump (BSEP) in Suspension Human Hepatocytes

Paresh P. Chothe[*1,2], Rachel Pemberton[1] and Niresh Hariparsad[1,3]

[1]Drug Metabolism and Pharmacokinetics, Vertex Pharmaceuticals Incorporated, Boston, Massachusetts, USA

[2]Current affiliation - Drug Metabolism and Pharmacokinetics, Takeda Pharmaceutical Company Limited, Cambridge, Massachusetts, USA

[3]Current affiliation – Drug Metabolism and Pharmacokinetics, AstraZeneca, 35 Gate House Park, Waltham, Massachusetts, USA

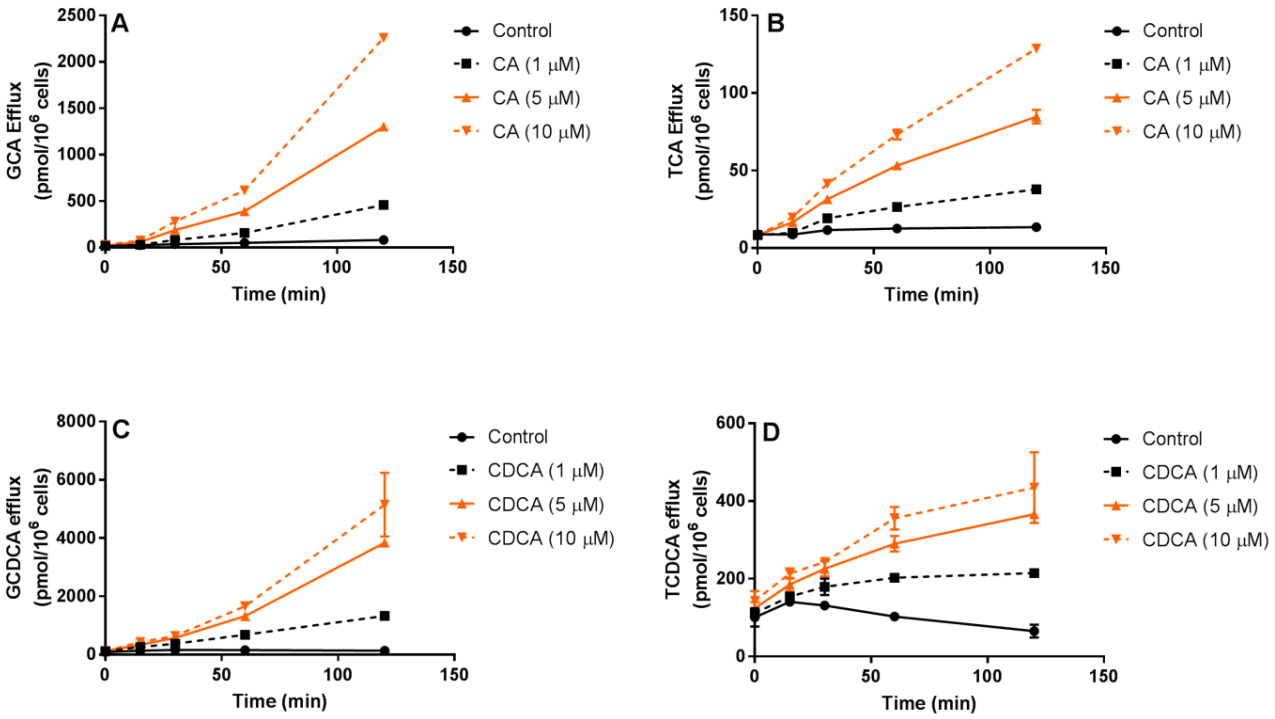

Supplemental Figure 1. Efflux of Glycine- and Taurine-conjugated CA and CDCA in Human Hepatocyte Suspension (WWQ). Cells were incubated with CA and CDCA at 1, 5 and 10 µM. Efflux of GCA (A), TCA (B), GCDCA (C) and TCDCA (D) was measured at 15, 30, 60 and 120 minutes. For control experiment cells were incubated with vehicle (DMSO <0.1%). The experiment was done in triplicate (n=3).

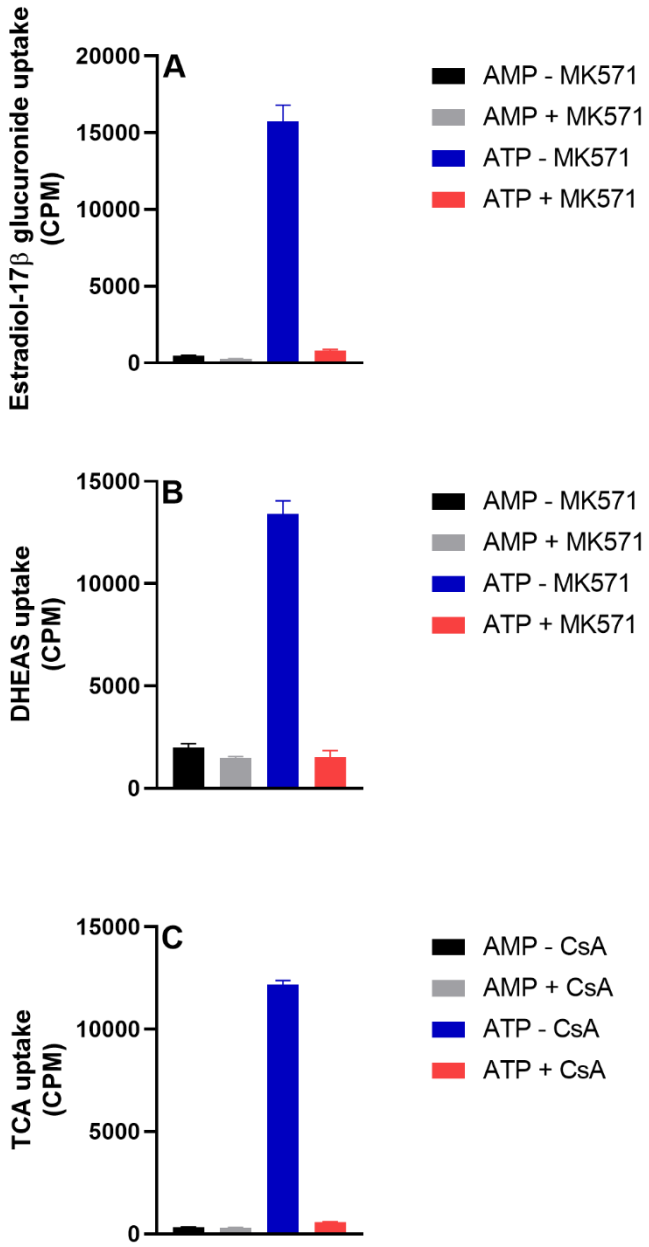

Supplemental Figure 2. Uptake Analysis of Estradiol-17β glucuronide, DHEAS and TCA in human MRP3, MRP4 and BSEP Overexpressed Membrane Vesicles, respectively. (A) Uptake of Estradiol-17β glucuronide (10 µM) was measured in the presence of AMP and ATP with and without MK571 (150 µM) in MRP3 overexpressed membrane vesicles. (B) Uptake of DHEAS (0.5 µM) was measured in the presence of

AMP and ATP with and without MK571 (150 µM) in MRP4 overexpressed membrane vesicles. (C) Uptake of TCA (0.2 µM) was measured in the presence of AMP and ATP with and without CsA (10 µM) in BSEP overexpressed membrane vesicles as described under method section. The experiment was done in triplicate (n=3).

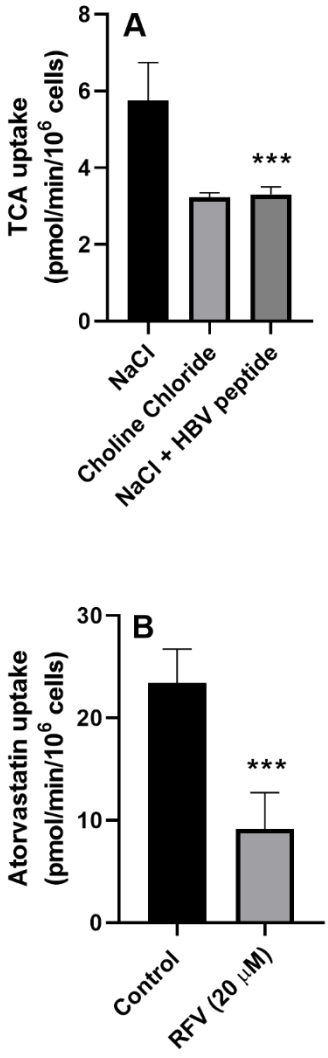

Supplemental Figure 3. Uptake Analysis of Taurocholate and Atorvastatin in Pooled Suspension Human Hepatocytes (YJG). (A) The uptake of taurocholate (2 μM) was measured in the presence of sodium-containing buffer (KHB buffer), sodium-free buffer (sodium chloride was replaced with choline chloride) and KHB buffer containing HBV peptide (0.1 μM) for 5 min. (B) The uptake of atorvastatin (0.5 μM) was measured in the absence and presence of 20 μM RFV for 3 min. The experiment was performed in triplicates (n=3). *** $p < 0.001$.

Supplemental Table 1. Demographic Information of Human Hepatocyte Donors

Donor ID	Donor	Sex	Age (year)	Race	Cause of death	BMI
WWQ	Single	Male	22	Caucasian	Head Trauma second to Blunt Injury	26.9
YZG	Pooled (5)	Mixed	NA	NA	NA	NA

Supplemental Table 2: The multiple Reaction Monitoring (MRM) Transitions of Compounds

Compound	Electrospray Ionization (ESI) mode	Parent Ion m/z	Fragment ion m/z	DP (V)	CE (V)
Atorvastatin	Positive	559.336	250.139	100	60
Bosentan	Positive	552.281	552.281	125	50
Estradiol 17β-glucuronide	Negative	447.3	113.1	-35	-36
Rifampicin	Positive	823.6	791.44	70	25
Troglitazone	Negative	440.203	397.197	-90	-30
Troglitazone sulfate	Negative	520	440	-49	-30
CA[1]	Negative	407.446	407.446	-145	-40
CDCA[2]	Negative	391.2	391.2	-170	-40
G-CA[3]	Positive	466.508	412.317	105	30
T-CA[4]	Positive	516.4	462.2	100	20
G-CDCA[5]	Positive	450.462	414.314	60	20
T-CDCA[6]	Positive	500.464	464.342	85	20

[1]cholic acid, [2]chenodeoxycholic acid, [3]glycocholic acid, [4]taurocholic acid, [5]glycochenodeoxycholic acid, [6]taurochenodeoxycholic acid.

Supplemental Table 3: Human transporter proteotypic heavy labeled tryptic peptide standards

Transporter (Gene)	**Peptide Sequence**	**MRMs 1 and 2 (product ion) [mass spectrometer specific]**
P-gp	I_{368}IDNKPSIDSYSK$_{380}$	496.60/631.32 (y11), 496.60/904.46 (y8)
MRP2	Y_{514}FAWEPSFR$_{522}$	606.79/902.44 (y7), 606.79/516.28 (y4)
MRP3	G_{654}ALVAVVGPVGCGK$_{667}$	646.37/682.35 (y7), 646.37/781.42 (y8)
OATP1B1	N_{321}VTGFFQSFK$_{330}$	591.81/969.50 (y8), 591.81/868.46 (y7)
OATP1B3	I_{615}YNSVFFGR$_{623}$	556.79/836.43 (y7), 556.79/722.34 (y6)
OATP2B1	Y_{641}YNNDLLR$_{648}$	540.77/754.41 (y6), 540.77/917.47 (y7)
OAT2	N_{20}VALLALPR$_{28}$	488.81/763.51 (y7), 488.81/579.39 (y5)
OAT7	D_{313}TLTLEILK$_{321}$	527.32/724.48 (y6), 527.32/837.56 (y7)
BSEP	S_{462}TALQLIQR$_{470}$	520.31/539.35 (y4), 520.31/667.41 (y5)
NTCP	G_{144}IYDGDLK$_{151}$	444.73/718.35 (y6), 444.73/555.29 (y5)
NaK ATPase	V_{213}DNSSLTGESEPQTR$_{227}$	543.92/511.29 (y4), 815.38/511.29 (y4)
GammaGTP	L_{156}FQPSIQLAR$_{165}$	591.85/794.48 (y7), 591.85/389.22 (b3)
OCT1	L_{330}SPSFADLFR$_{339}$	581.81/481.75 (y8), 581.81/865.44 (y7)
NaK ATPase	V_{213}DNSSLTGESEPQTR$_{227}$	543.92/511.29 (y4), 815.38/511.29 (y4)

Supplemental Table 4: Uptake data of Cholic Acid (CA) and Chenodeoxycholic Acid (CDCA) in Pooled Human Suspension Hepatocytes

Compound	Uptake (pmol/min/10^6 cells)		
	Control	**RFV (20 µM)**	**HBV peptide (0.1 µM)**
CA	1.22 ± 0.1	0.76** ± 0.08	0.69** ± 0.13
CDCA	6.84 ± 1.1	5.33 ± 0.74	5.60 ± 1.1

The data is presented as mean ± SD

** $p < 0.005$

Supplemental Table 5: Permeability of Cholic Acid (CA) and Chenodeoxycholic Acid (CDCA) and Their Glycine- and Taurine-conjugated Salts

	CA	CDCA	GCA	TCA	GCDCA	TCDCA
MDCK, Papp ($\times 10^{-6}$ cm/s)	0.1	3.7	0.1	0.3	0.3	0.4

Supplemental Table 6: Summary of Uptake Data of Bile Salts in MRP3 Membrane Vesicles

Bile salt	Uptake (pmol/mg)								fold change
	ATP				AMP				
	ATP - MK571		ATP + MK571		AMP - MK571		AMP + MK571		
	Mean	SD	Mean	SD	Mean	SD	Mean	SD	
GCA	64.69	2.23	5.26	0.87	11.86	0.92	5.86	0.06	5.45
TCA	26.35	0.29	5.8	0.49	12.04	0.35	5.28	0.21	2.18
GCDCA	195.52	4.56	17.6	0.42	36.56	1.92	15.55	0.43	5.35
TCDCA	80.96	3.15	18.71	0.53	32.99	0.81	16.9	1.87	2.45

Supplemental Table 7: Summary of Uptake Data of Bile Salts in MRP4 Membrane Vesicles

Bile Salt	Uptake (pmol/mg)								fold change
	ATP				AMP				
	ATP - MK571		ATP + MK571		AMP - MK571		AMP + MK571		
	Mean	SD	Mean	SD	Mean	SD	Mean	SD	
GCA	9.81	0.98	4.29	0.76	8.39	0.96	4.24	0.16	1.17
TCA	13.59	1.88	8.25	0.7	11.08	0.63	8.62	0.84	1.23
GCDCA	33.61	4.76	19.08	1.35	24.97	3.23	17.48	1.05	1.35
TCDCA	34.64	6.65	15.1	2.07	22.18	3.33	17.3	2.04	1.56

Supplemental Table 8: Summary of Uptake Data of Bile Salts in BSEP Membrane Vesicles

Bile salt	Uptake (pmol/mg)								fold change
	ATP				AMP				
	ATP - CsA		ATP + CsA		AMP - CsA		AMP + CsA		
	Mean	SD	Mean	SD	Mean	SD	Mean	SD	
GCA	299.08	9.71	15.81	0.85	7.17	1.15	7.08	0.67	41.72
TCA	617.48	27.6	44.66	2.57	20.05	4.68	17.85	3.33	30.80
GCDCA	255.08	22.38	84.17	32	22.01	1.25	16.58	2.67	11.59
TCDCA	323.71	22.15	94.69	15.42	27.79	2.60	29.37	5.72	11.65